Power Quality Enhancement in Grid-Connected Photovoltaic Systems Integrated with Shunt Active Power Filter Using Modulated Model Predictive Control

Nguyen Van Tan, Nguyen Huu Hieu, Luong Thanh Nhon, Tran Van Quoc, Nguyen Nhat Huu, Truong Thi Bich Thanh*, Nguyen Hong Viet Phuong
Faculty of Electrical Engineering
The University of Danang - University of Science and Technology
Da Nang, Viet Nam
tan78dhbk@dut.udn.vn, nhhieu@dut.udn.vn, 105220029@sv1.dut.udn.vn, 105210211@sv1.dut.udn.vn, 105220151@sv1.dut.udn.vn, nhvphuong@dut.udn.vn
*Corresponding author: ttbthanh@dut.udn.vn

***Abstract*—This paper proposes a modulated model predictive control (M2PC) method based on current control for a grid-connected photovoltaic (PV) system integrated with shunt active power filter (SAPF). In conventional finite control set model predictive control (FCS-MPC), the optimal switching state is selected at each sampling instant, which leads to a variable switching frequency and causes current ripple and DC-link voltage fluctuations due to the limited number of switching states. To overcome this issue, the proposed method introduces a vector modulation stage to improve control performance. The method is applied to a grid-connected PV system integrated with SAPF that can both supply active power and compensate harmonic currents caused by nonlinear loads. Simulation results under varying solar irradiance show that the proposed method reduces harmonic distortion and improves the stability of the DC-link voltage compared to FCS-MPC.**

Keywords-Model predictive control; harmonic; photovoltaic; power quality; active power filter.

I. INTRODUCTION

Currently, power electronic devices are rapidly developing and widely applied; however, this also leads to a significant increase in nonlinear loads [1], which are one of the main causes of harmonic components in modern power systems. As a result, the power quality of conventional power grids is degraded due to the increasing distortion caused by renewable energy sources and nonlinear loads. To address these challenges, various control strategies combined with power electronic converters have been proposed to improve the power quality of the system [2], [3], [4], [5]. Among them, the shunt active power filter (SAPF) has been widely used due to its fast dynamic response and robust operation under varying load conditions [6]. This paper proposes a grid-connected photovoltaic (PV) system integrated with SAPF, while maintaining efficient power conversion to the grid.

Model predictive control (MPC) is a control strategy that has been developed and applied since the 1970s in various industrial control systems [7]. In recent years, with the rapid development of power electronics, MPC has been increasingly adopted due to its ability to explicitly handle constraints and provide fast dynamic response [8]. Recently, MPC-based methods have been studied to improve harmonic compensation performance and reduce implementation costs [1], [5], [9], [10]. Among these methods, finite control set model predictive control (FCS-MPC) is one of the most widely used control strategies. This approach utilizes state-space model to predict system behavior, evaluates a finite set of switching states of the converter, and selects the most suitable state based on a cost function [11]. However, due to the absence of a modulation stage, the switching frequency is variable, which may increase current ripple and degrade current quality [12]. To address this limitation, a finite control set modulated model predictive control (FCS-M2PC) method based on reactive power compensation has been developed and applied to SAPF systems to enhance harmonic filtering performance compared to conventional FCS-MPC [13]. Unlike FCS-MPC, this method synthesizes the output voltage using adjacent voltage vectors within the same sector along with corresponding duty cycles, thereby improving voltage accuracy and reducing current oscillations. In this paper, an FCS-M2PC method based on direct current control is proposed to enhance harmonic filtering performance. The filter current reference is directly derived from the error between the desired grid current and the load current, enabling direct regulation of the harmonic components to be compensated while maintaining conversion efficiency between the PV system and grid.

The paper is organized into five sections. Section 2 presents the system configuration and the mathematical model of the grid-connected PV system integrated with SAPF. Section 3 describes the FCS-M2PC methods based on direct current control. Simulation results under varying solar irradiance conditions are presented in Section 4 to compare the performance of conventional FCS-MPC and FCS-M2PC. Finally, Section 5 concludes the paper.

II. SYSTEM CONFIGURATION AND MODELING

A. PV array

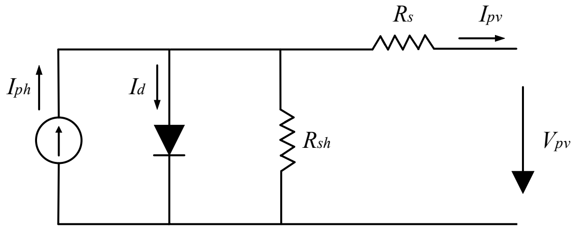

Figure 1. Equivalent circuit diagram of a PV cell

A PV array is composed of PV modules connected in series and parallel. Each module consists of multiple photovoltaic cells that convert solar energy into electrical energy, as shown in Fig. 1 [14]. The current generated by a PV cell is described as follows.

$$I_{PV} = I_{ph} - I_o \left\{ exp\left[\frac{q(V_{PV} + IR_s)}{nkT_c}\right] - 1 \right\} - \frac{V_{PV} + IR_s}{R_{sh}} \quad (1)$$

Where I_{ph} is the photocurrent generated by solar irradiance, I_o is the diode reverse saturation current, q is the electron charge, V_{PV} is the voltage of the PV cell, I is the cell current, n is the diode ideality factor.

B. DC/DC boost converter and P&O Algorithm for MPPT

The DC/DC boost converter consists of power electronic components, as shown in Fig. 2. The voltage generated by PV is fed into DC/DC boost converter, where it is stepped up and regulated to a DC-link reference value. The DC/DC boost converter applies maximum power point tracking (MPPT) algorithms by generating modulated switching signals to maximize the power extracted from the PV array [15], [16], [17].

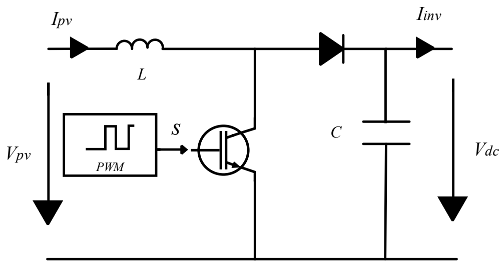

Figure 2. DC–DC boost converter topology

The relationship between the PV input voltage and the DC-link output voltage can be expressed as follows.

$$\frac{V_{dc}}{V_{pv}} = \frac{1}{1-D} \quad (2)$$

In this paper, the Perturb and Observe (P&O) algorithm is used due to its simplicity and ease of implementation in PV system. The P&O algorithm operates by observing the variation in power resulting from the PV voltage and current variable, thereby determining the direction to adjust the operating point toward the MPP. The operating principle of the algorithm is summarized in the flowchart shown in Fig. 3.

TABLE I. SWITCHING STATE AND VOLTAGE VECTOR

Voltage vector	Switching state		
	S_1	S_3	S_5
V_0	0	0	0
V_1	1	0	0
V_2	1	1	0
V_3	0	1	0
V_4	0	1	1
V_5	0	0	1
V_6	1	0	1
V_7	1	1	1

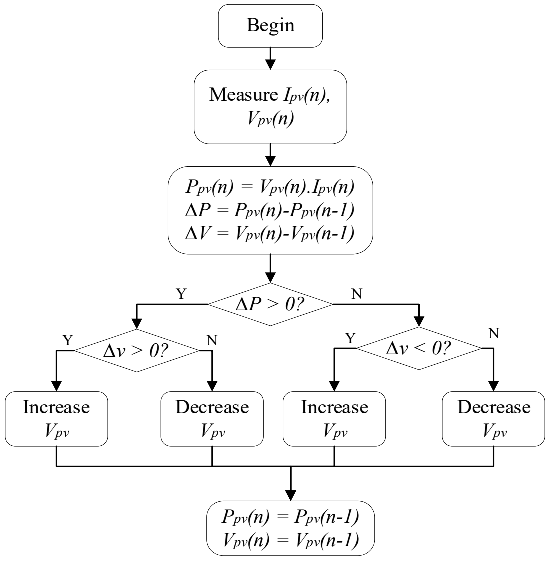

Figure 3. P&O Algorithm flowchart

C. Shunt active power filter

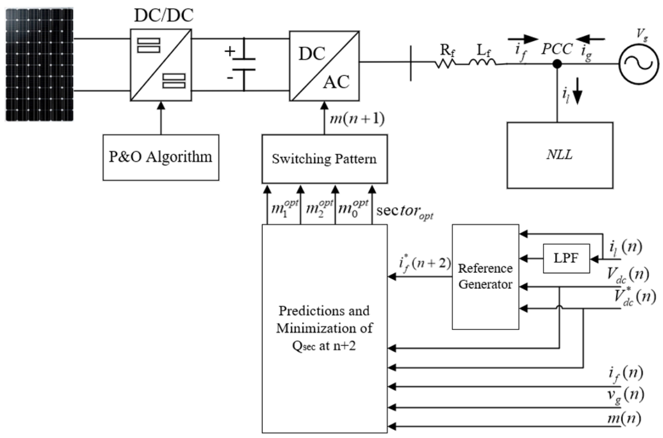

Figure 4. Scheme diagram of proposed system

The SAPF can be considered as an inverter interfacing AC grid and DC-link. In the proposed configuration, the DC-link is connected to the PV source, as shown in Fig. 4. In addition to harmonic current compensation to mitigate the impact of nonlinear loads on the grid, the SAPF also transfers the active power generated by PV system while maintaining DC-link voltage at its reference value. To simplify the model, a balanced three-phase system is assumed, and the effects of grid and nonlinear load impedances are neglected [13]. The current dynamics can then be expressed as follows.

$$\begin{cases} \dfrac{di_{fa}}{dt} = \dfrac{1}{L_f}V_{ga}(t) - \dfrac{R_f}{L_f}i_{fa}(t) - \dfrac{1}{3L_f}[2S_1(t) - S_3(t) - S_5(t)]V_{dc} \\ \dfrac{di_{fb}}{dt} = \dfrac{1}{L_f}V_{gb}(t) - \dfrac{R_f}{L_f}i_{fb}(t) - \dfrac{1}{3L_f}[2S_3(t) - S_1(t) - S_5(t)]V_{dc} \\ i_{fc}(t) = -[i_{fa}(t) + i_{fb}(t)] \end{cases} \quad (3)$$

$S_1(t)$, $S_3(t)$ and $S_5(t)$ are inverter switching states, R_f and L_f are the filter resistance and inductance, respectively. The DC-link voltage is given as follows.

$$\frac{dV_{dc}}{dt} = \frac{1}{C_{bus}}\{[S_1(t) - S_5(t)]i_{fa}(t) + [S_3(t) - S_5(t)]i_{fb}(t)\} \quad (4)$$

The grid-side current is expressed as follows.

$$\begin{cases} i_{ga}(t) = i_{la}(t) - i_{fa}(t) \\ i_{gb}(t) = i_{lb}(t) - i_{fb}(t) \\ i_{gc}(t) = -[i_{ga}(t) + i_{gb}(t)] \end{cases} \quad (5)$$

Equations (3), (4) are combined and discretized using the forward Euler method for controller design. The discrete-time state-space model of the system is given as follows.

$$\begin{cases} i_{fa}(n+1) = \left(1 - \dfrac{R_f T_s}{L_f}\right)i_{fa}(n) + \dfrac{T_s}{L_f}V_{ga}(n) - \dfrac{T_s}{L_f}X_1\overline{S}(n)V_{dc}(n) \\ i_{fb}(n+1) = \left(1 - \dfrac{R_f T_s}{L_f}\right)i_{fb}(n) + \dfrac{T_s}{L_f}V_{gb}(n) - \dfrac{T_s}{L_f}X_2\overline{S}(n)V_{dc}(n) \\ V_{dc}(n+1) = V_{dc}(n) + \dfrac{T_s}{C_{bus}}\overline{S}(n)Y_1 i_{fa}(n) + \dfrac{T_s}{C_{bus}}\overline{S}(n)Y_2 i_{fb}(n) \end{cases} \quad (6)$$

Where n denotes the discrete-time sampling instant, T_s is the sampling period, $\overline{S}(n)$, X_1, X_2, Y_1, Y_2 represent the switching state matrix and corresponding coefficient matrices, respectively, which are defined as follows.

$$\begin{gathered} \overline{S}(n) = [S_1(n) \quad S_3(n) \quad S_5(n)]^T \\ X_1 = \begin{bmatrix} \frac{2}{3} & \frac{-1}{3} & \frac{-1}{3} \end{bmatrix} \qquad X_2 = \begin{bmatrix} \frac{-1}{3} & \frac{2}{3} & \frac{-1}{3} \end{bmatrix} \\ Y_1 = [1 \quad 0 \quad -1] \qquad Y_2 = [0 \quad 1 \quad -1] \end{gathered} \quad (7)$$

III. MODULATED MODEL PREDICTIVE CONTROL BASED ON CURRENT CONTROL

A. Generate reference current for SAPF

To allow the cost function to evaluate the deviation from the reference value, thereby determining the optimal control input, the generation of a reference current is required. In PV integrated SAPF system, the reference grid current depends not only on the fundamental component of the load current but also on the power required to maintain the DC-link voltage. In the proposed configuration, the PV source can partially or fully supply the required power of the DC-link. However, when the PV power is insufficient, a DC-link charging current is required to regulate the DC-link voltage. The grid-side reference current is expressed as follows.

$$i^*_{sabc}(n) = i_{labc1}(n) + i_{dc}(n) \quad (8)$$

Where i_{labc1} is the fundamental component of the load current, i_{dc} is the instantaneous DC-link charging current, which is in phase with the grid voltage and whose amplitude I_{dc} is determined according to (9), assuming that inverter losses are neglected [18].

$$I_{dc} = \frac{2C_{bus}\{[V^*_{dc}(n)]^2 - [V_{dc}(n)]^2\}}{V_m T} \quad (9)$$

Where V_m is the peak value of the grid voltage, T is the period of the grid frequency. Finally, the reference filter current is defined as follows.

$$i^*_{fabc}(n) = i^*_{sabc}(n) - i_{labc}(n) \quad (10)$$

B. Modulated model predictive control

At the sampling instant n, the system state at n+1 is predicted based on the measured variables. Due to computational time delay, the control signal calculated at n is applied at n+1; therefore, the FCS-M2PC method employs a two-step prediction to estimate the system state at n+2 [13]. Unlike conventional FCS-MPC, which directly applies single switching states, the voltage vector at instant n is approximated by an equivalent voltage vector using duty cycles and voltage vectors within the optimal sector. This approach provides a more accurate synthesized voltage vector using the corresponding duty cycle as expressed below.

$$S_{eq}(n) = m_0(n)S_0(n) + m_1(n)S_1(n) + m_2(n)S_2(n) \quad (11)$$

Based on the established discrete-time model (6), the future state of the system at n+2 is predicted for each candidate switching state S(n+1) as shown in Table I, to evaluate the cost function. The two-step prediction model is formulated as follows.

$$\overline{X_P}(n+2) = A_2[S(n+1)]\overline{X}(n) + B_2[S(n+1)]\overline{U}(n) \quad (12)$$

Where A_2, B_2 are the equivalent discrete-time system matrices for the two-step prediction model, obtained by combining the system dynamics over two sampling periods and depending on the candidate switching state $S(n+1)$. The variables $\overline{X}(n)$ and $\overline{X}(n+2)$ denote the state variable vector at instants n and n+2, respectively, $\overline{U}(n)$ is the manipulated variable at instant n, as shown in (13).

$$\begin{cases} \overline{X}_p(n+2) = [i_{fa}(n+2) \quad i_{fb}(n+2) \quad V_{dc}(n+2)]^T \\ \overline{X}(n) = [i_{fa}(n) \quad i_{fb}(n) \quad V_{dc}(n)]^T \\ \overline{U}(n) = [V_{ga}(n) \quad V_{gb}(n)]^T \end{cases} \quad (13)$$

Due to the high switching frequency, the following expressions can be considered acceptable

$$\begin{cases} V_{dc}^{p}(n+2) = [0 \quad 0 \quad 1]\overline{X}_p(n+2) \\ i_{fabc}^{*}(n+2) = i_{fabc}^{*}(n) \end{cases} \tag{14}$$

First, the cost function is evaluated for each candidate voltage vector at instant n+1, as given in (14), where γ is a weighting factor that balances the different terms in the cost function.

$$\begin{aligned} Q_{S(n+1)} &= \gamma\left|V_{dc}^{*}(n+2) - V_{dc}^{p}(n+2)\right| \\ &+\left|i_{fa}^{*}(n+2) - i_{fa}^{p}(n+2)\right| + \left|i_{fb}^{*}(n+2) - i_{fb}^{p}(n+2)\right| \\ &+\left|i_{fc}^{*}(n+2) - i_{fc}^{p}(n+2)\right| \end{aligned} \tag{15}$$

Next, the cost function in (15) is evaluated for the three candidate voltage vectors in each sector in the αβ frame. The resulting cost values are then combined to compute the duty cycles m_0, m_1 and m_2, and to determine the overall cost of each sector. The sector that yields the minimum cost, along with its corresponding duty cycles, is selected as the optimal solution.

$$Q_{sopt}(n+1) = m_0 Q_0 + m_1 Q_1 + m_2 Q_2 \tag{16}$$

The duty cycles m_0, m_1 and m_2 are expressed as follows.

$$\begin{cases} m_1 = \dfrac{Q_0 Q_2}{Q_0 Q_1 + Q_0 Q_2 + Q_1 Q_2} \\ m_2 = \dfrac{Q_0 Q_1}{Q_0 Q_1 + Q_0 Q_2 + Q_1 Q_2} \\ m_0 = 1 - (m_1 + m_2) \end{cases} \tag{17}$$

Finally, the optimal duty cycles are applied to switching pattern block, where the switching sequence is formed using the voltage vectors of the optimal sector to generate the converter control signals [19].

IV. SIMULATION RESULT

To validate the effectiveness of the proposed algorithm in comparison with the conventional FCS-MPC method, simulations of the proposed system are carried out using MATLAB/Simulink. In this section, the algorithm is evaluated under varying solar irradiance to assess its harmonic compensation performance, and its ability to process power fluctuations caused by variations in solar irradiance. The system nominal parameters are first presented in Table II.

TABLE II. SYSTEM PARAMETERS

	Nominal parameter		
	Parameter	***Unit***	***Value***
Filter Inductor	L_f	mH	7.5
Filter Resistor	R_f	Ω	0.4
Rated DC Voltage	V_{dc}^{*}	V	700
DC-link Capacity	C_{bus}	mF	2.2
Rated PV power	P_{pv}	kW	4

A time-varying solar irradiance profile, as shown in Fig. 5, is applied in the simulation to evaluate the system performance under realistic operating conditions. Variations in irradiance lead to changes in the generated PV power, which directly affect the DC-link voltage as well as the grid-side variables.

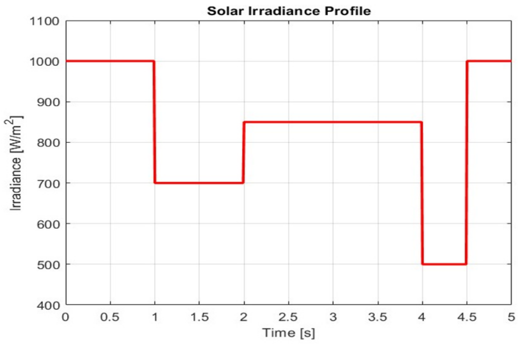

Figure 5. Solar irradiance profile

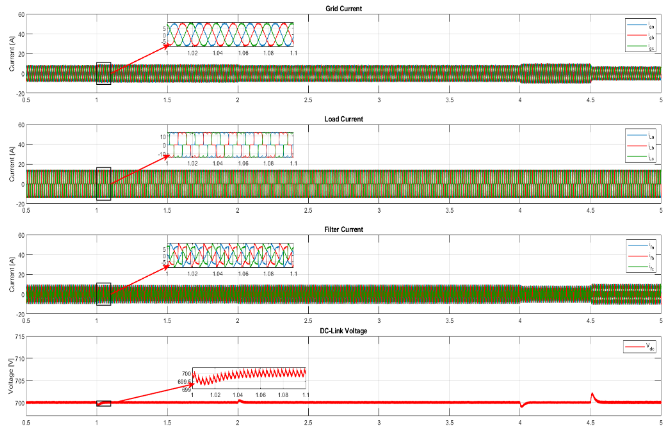

(a)

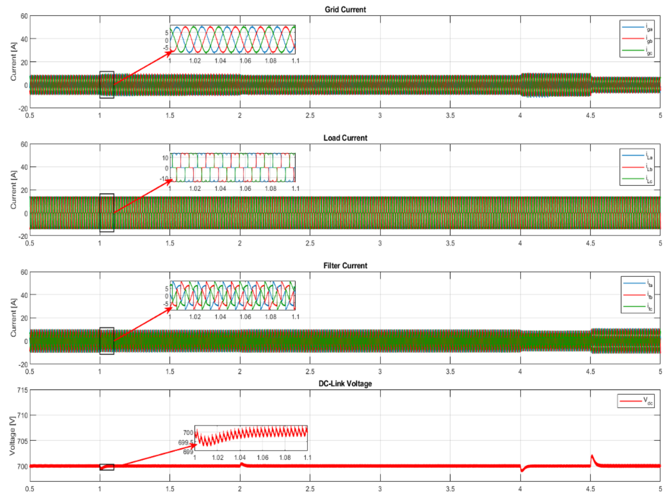

(b)

Figure 6. Simulation result of proposed system using (a) conventional FCS-MPC (b) FCS-M2PC

In terms of current waveforms, both methods maintain balanced three-phase grid currents and achieve effective harmonic compensation throughout the irradiance variation. However, FCS-M2PC leads to smoother grid current waveforms with significantly reduced high-frequency ripples compared to conventional FCS-MPC, as shown in Fig. 6. This improvement can be attributed to the fact that FCS-M2PC synthesizes the output voltage using multiple voltage vectors through duty cycles, rather than selecting a single switching state as in FCS-MPC. As a result, switching transients are reduced, leading to improved current tracking performance. Furthermore, the DC-link voltage exhibits better stability, as the power exchange between the AC and DC sides is more smoothly distributed by virtue of modulator, instead of depending on discrete switching states as in FCS-MPC. This contributes to improved energy regulation across the DC-link.

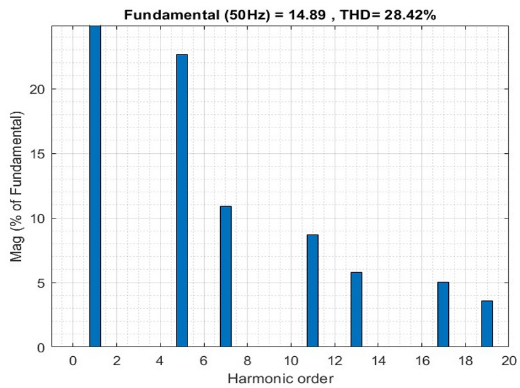

(a)

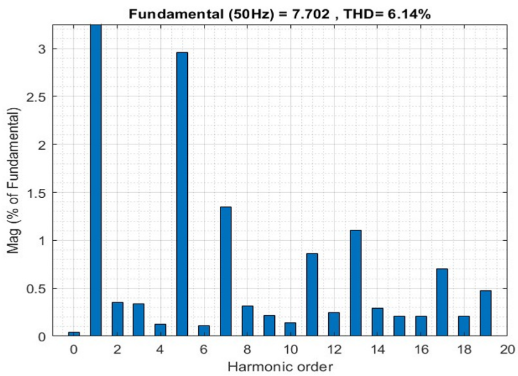

(b)

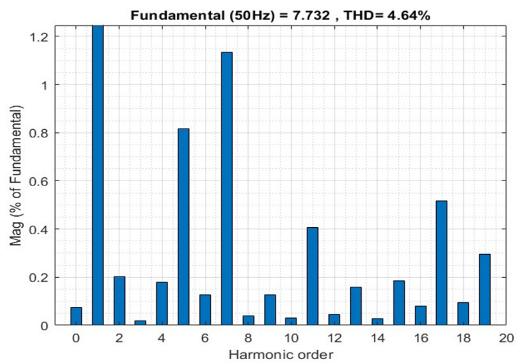

(c)

Figure 7. Grid current THD: (a) Before compensation (b) After compensation using conventional FCS-MPC (c) After compensation using FCS-M2PC

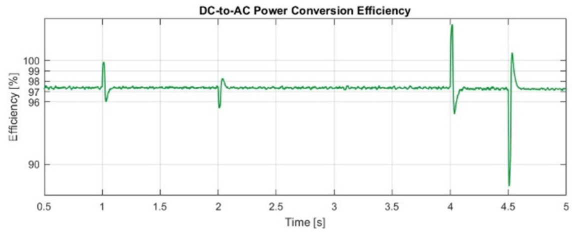

(a)

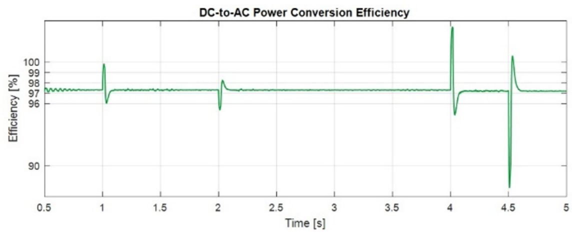

(b)

Figure 8. Conversion effienciency (a) conventional FCS-MPC (b) FCS-M2PC

Regarding the harmonic spectrum in Fig. 7, FCS-M2PC reduces the total harmonic distortion (THD) from 28.42% before compensation to 4.64%, which is lower than the 6.14% obtained with FCS-MPC in the same condition. The use of multiple voltage vectors through duty cycles enables the synthesized output voltage to more closely match the reference value, thereby improving current tracking performance and reducing control error within each sampling period, especially under varying irradiance conditions. However, due to the assumption that certain variables remain constant between consecutive sampling instants at high switching frequency, arising from computational delay, together with inaccuracies in extracting the fundamental component of the load current, even-order harmonic components appear after compensation.

Finally, the conversion effienciency of both methods reaches a high value of approximately 97.3%, as shown in Fig. 8. However, FCS-M2PC exhibits more stable performance with smaller fluctuations over time. Overall, the proposed method improves power quality and system stability mainly due to its ability to flexibly synthesize the output voltage vector and to mitigate the effects of single switching states, while maintaining comparable efficiency.

V. CONCLUSION

This paper has proposed an FCS-M2PC strategy based on current control for a grid-connected PV system integrated with shunt active power filter. The proposed controller enables the inverter to simultaneously transfer active power into the grid and compensate for harmonic currents caused by nonlinear loads. Simulation results under varying irradiance conditions are shown in the previous section, although both FCS-MPC and FCS-M2PC can maintain balanced grid currents and effective harmonic compensation, the proposed FCS-M2PC achieves better steady-state performance, including lower current THD and reduced DC-link voltage fluctuations. Specifically, the grid current THD is reduced from 28.42% before compensation to 4.64% using FCS-M2PC, compared to 6.14% with the conventional FCS-MPC, while both methods maintain an efficiency of approximately 97.3%. These results demonstrate that the proposed strategy is effective in improving power quality in multifunctional grid-connected PV systems.

References

[1] M. Popescu, A. Bitoleanu, C. V. Suru, M. Linca, and L. Alboteanu, "Shunt active power filters in three-phase, three-wire systems: A topical review," Energies, vol. 17, no. 12, p. 2867, Jun. 2024.

[2] W.-L. Chen, Z.-C. Li, and C.-Z. Xie, "Control of static synchronous compensator with supplementary damping enhancement for wind farm voltage regulation," IET Generation, Transmission & Distribution, vol. 5, no. 12, pp. 1211–1220, 2011.

[3] A. Hamadi, S. Rahmani, and K. Al-Haddad, "Novel hybrid series active filter for power quality compensation," in Proc. IEEE Power Electron. Spec. Conf. (PESC), Orlando, FL, USA, 2007, pp. 1099–1104.

[4] A. Hamadi, S. Rahmani, and K. Al-Haddad, "A hybrid passive filter configuration for VAR control and harmonic compensation," IEEE Trans. Ind. Electron., vol. 57, no. 7, pp. 2419–2434, Jul. 2010.

[5] Amrani, Z.; Beladel, A.; Kouzou, A.; Rodriguez, J.; Abdelrahem, M. Four-Wire Three-Level NPC Shunt Active Power Filter Using Model Predictive Control Based on the Grid-Tied PV System for Power Quality Enhancement. Energies 2024, 17, 3822.

[6] R. Kumar and H. O. Bansal, "Shunt active power filter: Current status of control techniques and its integration to renewable energy sources," Sustainable Cities and Society, vol. 42, pp. 574–592, Oct. 2018.

[7] L. Wang, Model Predictive Control System Design and Implementation Using MATLAB. London, U.K.: Springer, 2009.

[8] A. A. Ghany, E. G. Shehata, A.-H. M. Elsayed, Y. S. Mohamed, H. H. Alhelou, P. Siano, and A. A. Z. Diab, "Novel switching frequency FCS-MPC of PMSG for grid-connected wind energy conversion system with coordinated low voltage ride through," Electronics, vol. 10, no. 4, p. 492, Feb. 2021.

[9] A. A. Abdel-Aziz, M. A. Elgenedy, and B. W. Williams, "Model predictive current control for low-cost shunt active power filter," CSEE Journal of Power and Energy Systems, vol. 10, no. 4, pp. 1589–1598, Jul. 2024.

[10] D. Naamane, H. Benbouhenni, A. Chebabhi, Z. Laid, D. Zellouma, and I. Colak, "A new nonlinear control to improve the efficiency of the PV-SAPF system," Energy Reports, vol. 11, pp. 3096–3116, Mar. 2024.

[11] J. Rodriguez and P. Cortes, Predictive Control of Power Converters and Electrical Drives. Chichester, U.K.: Wiley, 2012.

[12] J. Rodriguez, M. P. Kazmierkowski, J. R. Espinoza, P. Zanchetta, H. Abu-Rub, H. A. Young, and C. A. Rojas, "State of the art of finite control set model predictive control in power electronics," IEEE Trans. Ind. Electron., vol. 56, no. 6, pp. 2226–2238, Jun. 2009.

[13] L. Tarisciotti, A. Formentini, A. Gaeta, M. Degano, P. Zanchetta, R. Rabbeni, and M. Pucci, "Model predictive control for shunt active filters with fixed switching frequency," IEEE Trans. Ind. Appl., vol. 53, no. 1, pp. 296–304, Jan./Feb. 2017.

[14] M. G. Villalva, J. R. Gazoli, and E. R. Filho, "Comprehensive approach to modeling and simulation of photovoltaic arrays," IEEE Trans. Power Electron., vol. 24, no. 5, pp. 1198–1208, May 2009.

[15] C. R. Algarín, J. T. Giraldo, and O. R. Álvarez, "Fuzzy logic based MPPT controller for a PV system," Energies, vol. 10, no. 12, p. 2036, Dec. 2017.

[16] K. Sundareswaran, V. Vignesh Kumar, and S. Palani, "Application of a combined particle swarm optimization and perturb and observe method for MPPT in PV systems under partial shading conditions," Renewable Energy, vol. 75, pp. 308–317, 2015.

[17] T. Esram and P. L. Chapman, "Comparison of photovoltaic array maximum power point tracking techniques," IEEE Trans. Energy Convers., vol. 22, no. 2, pp. 439–449, Jun. 2007.

[18] M. A. A. M. Zainuri, M. A. M. Radzi, A. C. Soh, N. Mariun, and N. A. Rahim, "DC-link capacitor voltage control for single-phase shunt active power filter with step size error cancellation in self-charging algorithm," IET Power Electron., vol. 9, no. 2, pp. 323–335, 2016.

[19] L. Tarisciotti, P. Zanchetta, A. Watson, J. Clare, M. Degano, and S. Bifaretti, "Modulated model predictive control (M2PC) for a 3-phase active front-end," in Proc. IEEE, 2013, pp. 1062–1069.